

## Microstructural and Electronic Properties of $\text{In}_3\text{Te}_4$ Single Crystals

G. A. Gamal <sup>1\*</sup> and M. Abou Zied <sup>2</sup>, A.A Ebnalwaied <sup>2</sup>

<sup>1</sup> College of Engineering - Qassim University- KSA

<sup>2</sup> Physics Department, Faculty of Science, South Valley University, Qena 83523, Egypt

Received 3/4/2012; accepted for publication 17/12/2012)

**Abstract.** X-ray line profile analysis was applied to obtain structural parameters (crystal lattice, grain size, micro-strain, dislocation density, dislocation arrangement, and the distance between two dislocations) of  $\text{In}_3\text{Te}_4$  crystals. The samples were prepared by a special modification of vertical Bridgman -Stockbarger technique. This method was examined for the first time. The Bragg peak line shapes of  $\text{In}_3\text{Te}_4$  crystals were analyzed using Scherrer equation, Williamson – Hall plot, and Warren - Averbach method. The effect of dislocation density on carrier mobility and carrier concentration was checked. We concluded that the grown crystal is tetragonal  $\text{In}_3\text{Te}_4$  crystal. The lattice parameters of the tetragonal  $\text{In}_3\text{Te}_4$  have been calculated from (013), (020), (113), (015), (220), (222), (132), (332), (242), and (244) reflection planes. The density of dislocations, the average distance between the adjacent dislocation, the dislocation arrangement parameter, Hall mobility and carrier density have the values:  $1.6 \times 10^{-14} \text{ m}^{-2}$ , 8.27 nm, 0.177,339  $\text{Cm}^2/\text{V} \cdot \text{Sec}$ ,  $1.35 \times 10^{14} \text{ Cm}^{-3}$  respectively.

**Keywords:**  $\text{In}_3\text{Te}_4$ , Crystal growth, Semiconductors, Lattice parameters, Dislocation density, Crystallite size, Micro strain, Hall Mobility.

## 1. Introduction

From the diagram based on thermal – analysis data due to W. Klemm *et al.* [1] it was stated that besides the phases  $\text{In}_2\text{Te}$ ,  $\text{InTe}$  and  $\text{In}_2\text{Te}_3$ , there is a higher telluride, which was not identified. It is evident from the In – Te phase diagram, which is redrawn from Shunk [2] that it contains  $\text{In}_3\text{Te}_4$ ,  $\text{InTe}$ ,  $\text{In}_2\text{Te}_3$ ,  $\text{In}_3\text{Te}_5$ ,  $\text{In}_2\text{Te}_5$  and  $\text{In}_9\text{Te}_7$  phases. There was a dispute about the structure of  $\text{In}_3\text{Te}_4$  where some authors showed that it is a rhombohedral structure with  $a = 4.26 \text{ \AA}$  and  $c = 40.6 \text{ \AA}$  [3] but others [4] said that  $\text{In}_3\text{Te}_4$  is a tetragonal structure with  $a = 6.173 \text{ \AA}$  and  $c = 12.438 \text{ \AA}$ .

The diffraction data of  $\text{In}_3\text{Te}_4$  in the form of thin films was studied earlier [5]. There are two major approaches for measuring the microstructure properties in crystalline materials. They are direct imaging using transmission electrons - microscopy (TEM) and indirect measurement using X-ray diffraction pattern (XRD). The study of line – broadening of X-ray Bragg reflections of deformed crystals has recently been developed in theory [6, 7] and in experiment [8–10] to a considerable extent and has been shown to be suitable to obtain dislocation densities that correlate well with TEM data. The technique is less direct than TEM but has the advantage that it can be applied to macroscopic volumes of bulk material. It is complementary to TEM in so far as it provides reliable information especially for high dislocation densities that are not easily investigated by TEM.

The present study was undertaken in order to grow  $\text{In}_3\text{Te}_4$  single crystals, investigate the grain size and microstructure properties of it by using the X-ray diffraction technique, and study the relation between microstructure and the electronic properties of  $\text{In}_3\text{Te}_4$  crystal.

## 2.

### Experimental

#### 2-1. Crystal Growth

It is known that in the Bridgman technique the melt is contained in crucible and progressively frozen to yield a single crystal if the rate of the movement is very low. However, the main problem in such technique is the absence of the smooth and accurate graduation of temperature, which is the main reason for coherent and incoherent precipitates. The present design is a modification of the traveling solvent method (TSM) technique, which is considered in the current work. The apparatus used for TSM) growth in this experiment is shown in Fig. (1). The main advantage of this technique is that the temperature gradient is granted by this simple design more details about this technique see ref. [11].

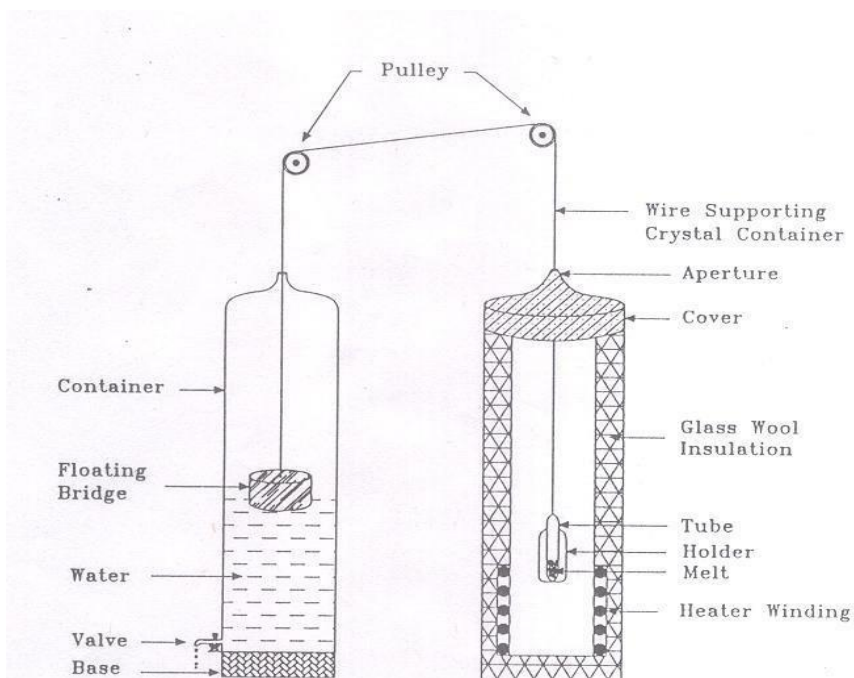


Fig. (1). Design of the new modification for crystal growth.

## 2-2. X-Ray Diffraction Technique

The X-ray diffractograms were measured stepwise with angle / second value of  $0.02^\circ$  at ambient temperature with a model D 5000 Siemens diffractometer (Germany). The instrument is equipped with a copper anode generating Ni filtered  $\text{CuK}\alpha$  radiation  $\lambda = 1.5406 \text{ \AA}$ , 40 kV, 30 mA, backmonochromator). The equipment was used in a  $\theta - 2\theta$  geometry in the range between  $10$  and  $80^\circ$  with a divergence slit of  $1^\circ$ . An on – line data acquisition and handling system facilitated an automatic JCPDS library search and match Diffract AT software, Siemens) for phase identification purpose. In the present, work we will show how we can utilize of X-ray pattern for determination of many important parameters.

## 3. Results and Discussion

### 3-1. Determination of Crystal Lattice

Fig. (2) shows the powder diffractogram of the  $\text{In}_3\text{Te}_4$  sample. In this figure, we can see strong Bragg peaks of X-ray diffraction pattern which indicate that the sample is crystalline. From the position of the strong peaks d-space has been calculated according to Bragg law:  $n\lambda = 2d \sin \theta$ .

The calculated values of  $d$  - spaces for different reflection planes are listed in table (1).

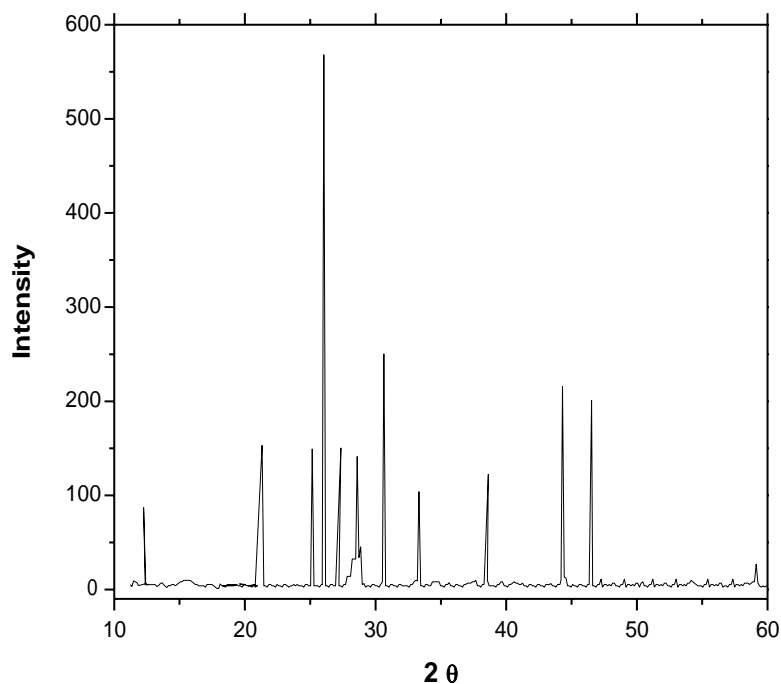


**Fig.(2).** The powder diffractogram of the  $\text{In}_3\text{Te}_4$  single phase crystal.

From table (1) we concluded that the main phase of the crystal is the tetragonal  $\text{In}_3\text{Te}_4$ . This was done where the  $d$  - spaces of the investigated sample correspond to the  $d$  - spaces that listed in the ASTM card for the tetragonal  $\text{In}_3\text{Te}_4$ . The lattice parameter of the tetragonal  $\text{In}_3\text{Te}_4$  has been calculated from 013), 020), 113), 015), 220), 222), 132), 332), 242), and 244) reflections according to the following equation [12]:

$$1/d^2_{hkl} = h^2 + k^2 / a^2 + l^2 / c^2$$

In this way values of the lattice parameters  $a$  and  $c$  of the tetragonal  $\text{In}_3\text{Te}_4$  of the different reflection planes were calculated .

**Table (1).** Comparison between  $d$  –  $space$  value of grown sample and  $d$  –  $space$  of the tetragonal  $\text{In}_3\text{Te}_4$ .

| $h\ k\ l$ | d-space of the grown sample<br>as calculated) | d- space of tetragonal $\text{In}_3\text{Te}_4$<br>as reported in the ASTM card ) |
|-----------|---|---|
| 013       | 3.464   | 3.47  |
| 020       | 3.122   | 3.11  |
| 113       | 2.99  | 3.02  |
| 015       | 2.317   | 2.305   |
| 220       | 2.158   | 2.16  |
| 222       | 2.046   | 2.06  |
| 132       | 1.87  | 1.858   |
| 332       | 1.416   | 1.414   |
| 242       | 1.354   | 1.353   |
| 244       | 1.245   | 1.25  |

In order to obtain the lattice parameters  $a$  and  $c$  of the tetragonal  $\text{In}_3\text{Te}_4$  substantially free from experimental error, one should plot the apparent values of  $a$  and  $c$  respectively against the corresponding values of the famous extrapolation

function  $F\theta$ ) which is:  $F(\theta) = \frac{\cos^2 \theta}{\sin \theta} + \frac{\cos^2 \theta}{\theta}$  [13]. Fig. (3) shows the relation

between the lattice parameter  $a$  and  $F\theta$ ). The interception of the extrapolation of straight line with y - axis gives the value of the lattice parameter  $a$ . The results indicate that the mean values of lattice parameter  $a = 6.184 \text{ \AA}$ . Fig. (4) shows the relation between the lattice parameter  $c$  and  $F\theta$ ). From the figure we could estimate the value of the lattice parameter  $c$  as  $12.43 \text{ \AA}$ . It must be mentioned that the investigated values of the lattice parameters  $a$  and  $c$  of our crystal are in a good accordance with the lattice parameter of the tetragonal  $\text{In}_3\text{Te}_4$ , which are published previously [4] where  $a = 6.173 \text{ \AA}$  and  $c = 12.438 \text{ \AA}$ .

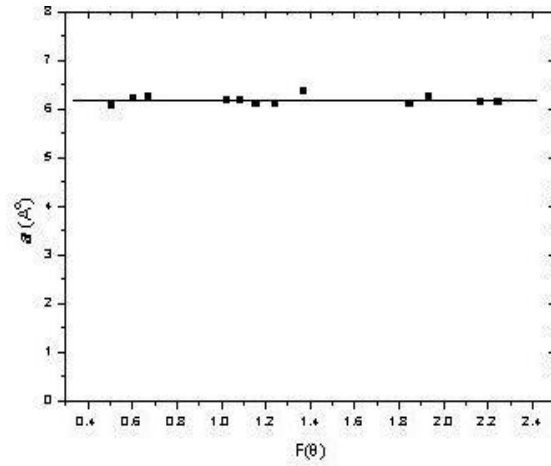


Fig. (3). The relation between the lattice parameter  $a$  and the extrapolation function  $F\theta$

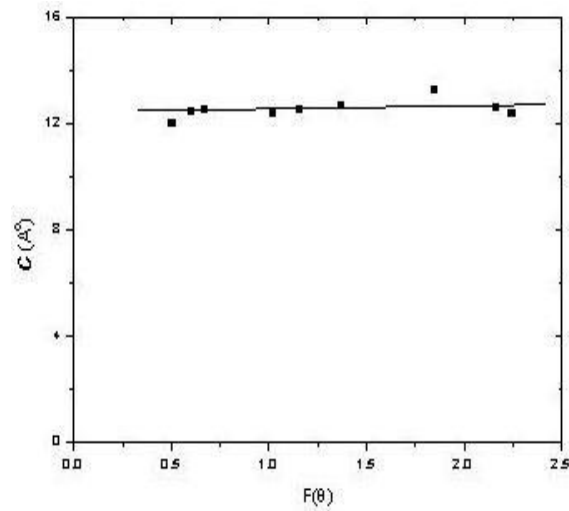


Fig. (4). The relation between the lattice parameter  $c$  . and the extrapolation function  $F$

### 3-2. Determination of Crystallite Size

From the Scherrer equation [14] we can obtain that the crystallite size  $D_{vol}$ ) for the tetragonal  $\text{In}_3\text{Te}_4$  crystal .It is 95.8 nm.

Also the Williamson-Hall equation can be given as [15]:

$$\Gamma \cos \theta = 0.9 \lambda / D_{vol} + 4 \varepsilon \sin \theta$$

Where  $\Gamma$  is the full width at half-maximum of x-ray peak at diffraction angel  $\theta$  , and  $\varepsilon$  is the micro-strain. Fig. (5) shows the Williamson-Hall plot of the tetragonal  $\text{In}_3\text{Te}_4$ . From the figure we can concluded that:

- $D_{vol} = 93.75 \text{ nm}$ .
- The increase of  $\Gamma \cos \theta / \lambda$  with  $\sin \theta / \lambda$  indicates the presence of lattice distortions, however, the deviation from the linear correlation corresponds to the anisotropy.

From the results of crystallite size measurements of specimen we can note that an average crystallite size measured by Scherrer equation is larger than that obtained from Williamson-Hall plot. Thus, apparently, the Scherrer method overestimates the grain size likely due to the fact that it does not separate broadening due to strain in the lattice from that due to refined grain structure [16].

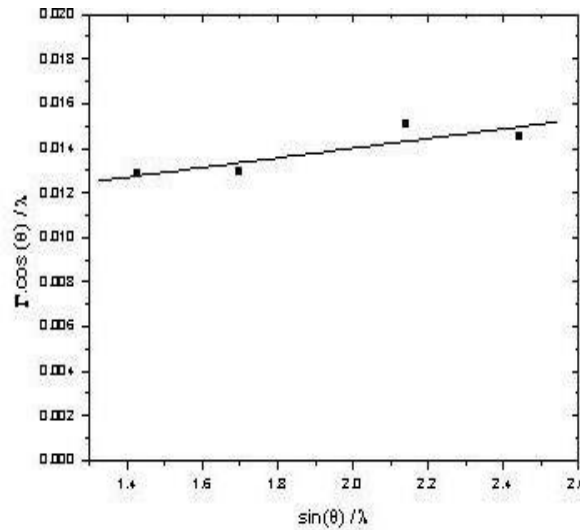


Fig. (5). Williamson-Hall plot of the tetragonal  $\text{In}_3\text{Te}_4$ .

### 3-3. Determination of Dislocations Parameters

Strain anisotropy is well known in X-ray line-broadening [17]. Several models have been suggested for it. A dislocation model has been suggested recently [18] that based on the anisotropic contrast of dislocations in diffraction [19]. In strained semiconductor structure dislocations produce peak shift and peak broadening [20]. The Warren – Averbach [21] is a Fourier method used to consider the separation of size and strain effects. The critical step is the Fourier transformation, which is very sensitive to statistical fluctuations in the data, to truncation effects, and to background

level. Therefore – for the original Warren – Averbach method – extremely good counting statistics and a wide angular measuring range are necessary.

The real part of the Fourier coefficients  $A_L$  can be given as the product of a purely size – broadening term  $S$ ) and a purely distortion – broadening term  $D$ ):

$$A_L = A_L^S \cdot A_L^D \quad \text{or} \quad \ln A_L = \ln A_L^S + \ln A_L^D$$

The distortion line broadening coefficients can be written as [22]:

$$\ln A_L^D = - \rho \pi b^2 / 2) L^2 \ln R_e / L) k^2$$

where  $L$  is the distance between two cells in a real space, and  $k$  is the diffraction vector. The basic equation of the Warren and Averbach analysis is obtained as [23]:

$$\ln A_L = \ln A_L^S - \rho \pi b^2 / 2) L^2 \ln R_e / L) k^2$$

where  $\rho$  and  $R_e$  are the dislocation density and the outer cut – off radius respectively.

The logarithms of the real part of the Fourier coefficients of different reflections for the tetragonal  $\text{In}_3\text{Te}_4$  crystal are plotted in Fig. (6) vs.  $k^2$ . From the figure we can note that the value of  $\ln A_L$  decreases with  $k^2$  on a global scale, indicating the presence of lattice distortions. Nevertheless, this behavior reflects the strong strain anisotropies.

Denoting the slope of the curve with  $S(L)$  we can get the equation:

$$S(L) / L^2 = \rho \pi b^2 / 2) \ln R_e) - \rho \pi b^2 / 2) \ln L)$$

Fig. (7) shows the relation between  $S(L) / L^2$  and  $\ln L$ , so we can get the dislocation density and the effective outer cut-off radius of dislocations  $R_e$ ). The average distance between the adjacent dislocations  $L_C$  and the dislocation arrangement parameter  $M$  are also calculated see table (2).

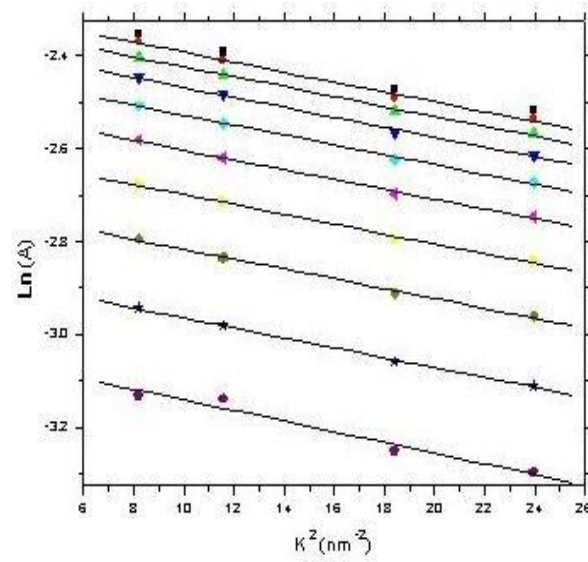


Fig. (6). The real part of the Fourier coefficients of the tetragonal  $\text{In}_3\text{Te}_4$  vs.  $k^2$ .

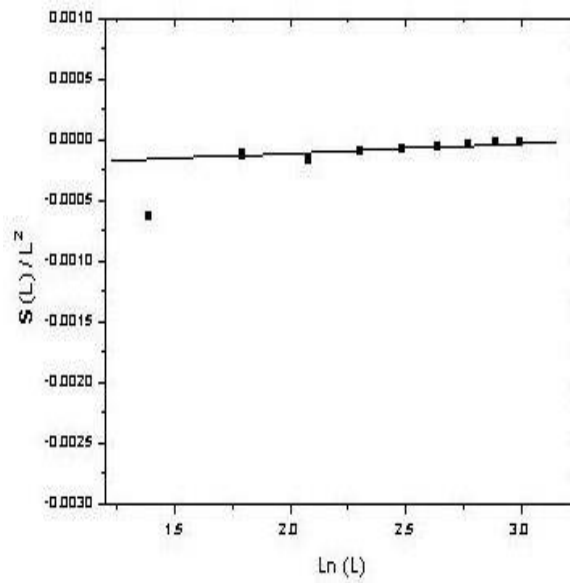


Fig. (7). The relation between  $(S L / L^2$  and  $\ln L$ ).

Table (2). Dislocation parameters for the tetragonal  $\text{In}_3\text{Te}_4$ .

| $\rho \text{ m}^{-2}$ | $L_c \text{ nm}$ | $R_c \text{ nm}$ | $M$   | Method          |
|-----------------------|------------------|------------------|-------|-----------------|
| $1.6 \times 10^{-14}$ | 7.9              | 14.05            | 0.177 | Warren–Averbach |

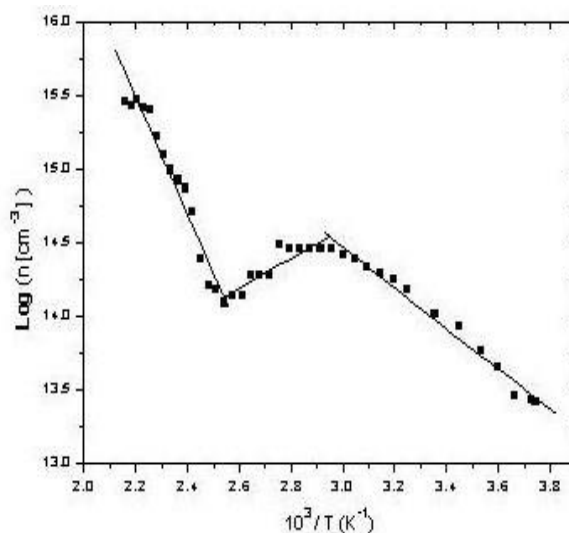
### 3.4 Determination of carrier mobility and carrier concentration

The present work has been dealt with investigation of the effect of temperature on the Hall mobility. The Hall mobility values were calculated according to the formula  $\mu = R_h \sigma$ . Both the Hall coefficient  $R_h$  and the electrical conductivity  $\sigma$  data have already been published [24]. From Fig. (8) illustrate this dependence for  $\text{In}_3\text{Te}_4$  sample. From the graph we have that:

$$\mu = 339 \text{ cm}^2 / \text{V. Sec.}$$

The general behavior of  $\mu$  against  $T$  can be divided into three regions: -

- 1-  $T < 338 \text{ K}$  the low temperature part) which corresponds to the extrinsic conduction.
- 2- The middle region  $338 \text{ K} < T < 402 \text{ K}$  which represent the transition region.
- 3- The high temperatures part  $T > 402 \text{ K}$  which is the intrinsic conduction part.

Fig. (8). Behavior of carrier concentration as a function of temperature for the tetra  $\text{In}_3\text{Te}_4$ .

The mobility in the low temperatures is governed by the law  $\mu \propto T^n$ . In our case the exponent  $n$  is abnormal because it is not positive as one expect, and it has the value -4.8), so we can write the law that governed mobility as:

$$\mu \propto T^{-4.8}.$$

In the high temperature side where the temperature coefficient is negative, the relation between mobility and temperature can be written as  $\mu \propto T^{-m}$ . In the present work the value of  $m$  is 12 which is high if compared to other semiconductors [25,26] .

Variation of the carrier density versus reciprocal temperature is shown in Fig. (9). At low temperatures below 338 K), the number of ionized donors determines the carrier concentration. At high temperatures the crystal is exhibiting an intrinsic behavior. The expected value for the intrinsic concentration could be given by the relation: -

$$N_i = 2(2\pi k / h^2)^{3/2} (m_n^* m_p^*)^{3/4} T^{3/2} \exp(-E_g / 2kT)$$

where  $m_n^*, m_p^*$  are the effective masses of both electron and hole respectively. Utilization of this formula leads to calculation of the energy gap width of  $\text{In}_3\text{Te}_4$ . It was computed as 1.71 eV. Finally the charge carriers concentration at room temperature, equals to  $1.35 \times 10^{14} \text{ cm}^{-3}$  in  $\text{In}_3\text{Te}_4$  crystal.

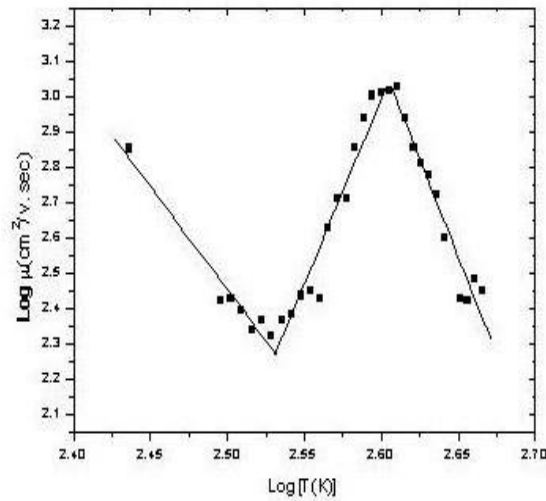


Fig. (9). Behavior of Hall mobility as a function of temperature for the tetragonal  $\text{In}_3\text{Te}_4$ .

If we compare the values of carrier mobility and carrier concentration of  $\text{In}_3\text{Te}_4$  crystal with the values of other semiconductors [24, 25, 26], we'll see that the values estimated for the  $\text{In}_3\text{Te}_4$  crystal are lower than the published values for other semiconductors.

If we look to the value of dislocation density of  $\text{In}_3\text{Te}_4$  crystal we'll find that it is very high if it compared with the semiconductors values [27, 28]. In our opinion the drop of the mobility and carrier concentration returns to the high value of dislocation density in  $\text{In}_3\text{Te}_4$  crystal. Dislocations are usually regarded as a capture centers to the carriers, so the mobility and carrier concentration are lower than other semiconductors.

#### 4. Conclusion

Single crystal of  $\text{In}_3\text{Te}_4$  has been prepared by the modified vertical Bridgman Stockbarger technique. The grain size, micro strain, character of dislocations, mobility and carrier concentration of the tetragonal  $\text{In}_3\text{Te}_4$  single crystal was determined. It has been found that:

- 1 The values of  $d$  – space of our sample show that it has a tetragonal structure.
- 2 The values of lattice parameters of the tetragonal  $\text{In}_3\text{Te}_4$  are in very satisfactory agreement with results obtained on similar crystals by other authors [4].
- 3 The evaluation method of X-ray line profile analysis applied in this work is capable of providing important microstructure parameters of the tetragonal  $\text{In}_3\text{Te}_4$  like crystallite size, micro strain, dislocation density and the average distance between adjacent dislocations).
- 4 The arrangement parameter  $M$  characterizing the effectiveness of the screening of neighboring dislocations was obtained from the X-ray line profile. The value of  $M$  gives the strength of the dipole character of dislocations. If  $M$  is small or large the dipole character and the screening of the displacements field of dislocations is strong or weak, respectively. At the same time, strong or weak screening and small or large values of  $M$  mean strong or weak correlation in the dislocation distributions, respectively.
- 5 Carrier mobility and carrier concentration was lower than other semiconductors due to high value of dislocation density.

#### 5. References

- [1] Klemm, W. and Vogel, H. U. V., "Z. anorg. Chem.," Vol. 219, 1934), pp. 45-64.
- [2] Shunk, F. A., "Constitution of Binary Alloys", second supplement, McGraw-Hill, New York, or General Electric Co., Business Growth Services, Schenectady, New York, 1969).
- [3] Geller S., Jayarman, A. and Hull W., "Journal of Physics and Chemistry of Solids", Vol. 26, No. 2, 1965), pp. 353-361.
- [4] Karakostas Th., Flevairs, N. F., Vlachavas, N., Bleris, G. L and Economou, N. A., "Acta Cryst", Vol. A34, 1978), pp.123-133.
- [5] Tolutis, V., Deksnys A., Paukste, J. and Verkelis, J., "Lietuvos Fizikos Rinkiny", Vol. 7, No. 2, 1967), pp.453-46.

- [6] Smith, R. A., "Semiconductors", Cambridge VP, 1961).
- [7] Gutmann, F. and Lyons, L. E., "Organic Semiconductor", John Wiley & Sons, Inc., New York. London. Sydney, 1967).
- [8] Crowford Dunlap, W., "An Introduction to Semiconductors", New York, 1957).
- [9] Kireev, P. S., "Semiconductors Physics", Mir publishers, Moscow, 1978).
- [10] Pascoe, K. G., "Solid State Physics c", Mir publishers, Moscow, 1979).
- [11] Gamal, G. A, Abou Zied, M. and Ebnalwaled, A. A, "*Chin. Phys. Lett.*", Vol. 22, No. 6 2005) pp.1530-1532.
- [12] Xiao, S. Q. and Gleiter, A. H "*Acta, Met. Mat.*," Vol. 42, 1994), pp.253-2542.
- [13] Varin, R. A., Bystrzycki, J. *Calka, Intermetallics*, Vol. 7, 1999), pp. 917-921.
- [14] Scherrer, P., *Gottinger Nachrichten*, Vol. 2, 1918), pp. 98-107.
- [15] Williamson, G. K and Hall, W. H., "*Acta Met.*", Vol. 1, 1953), pp.22-28.
- [16].Choudry, M. S, Dollar, M. and Eastman, J. A., "*Materials Science Engineering*", Vol.A-256, 1998), pp.25-30.
- [17] Caglioti, G., Paoletti, A. and Ricci, F. P., "*Nucl. Instrum.*", Vol. 3, 1958), pp.223-226.
- [18] Ungar, T. and Borbely, A., "*Appl. Phys. Letters*", Vol. 69, 1996), pp.3173-2179.
- [19] Wilkens, M., "*Phys. Stat. Sol. a)*", Vol. 2, 1970), pp.359-263.
- [20] Jesser, W. A. and Kuhlmann-Wilsdorf, D., "*Phys. Stat. Sol.*", Vol. 19, 1967), pp. 95-99.
- [21] Warren, B. E. and Averbach, L. E., "*J. Appl. Phys.*", Vol. 23, 1952), pp.497-505.
- [22] Groma I., Ungar, T. and Wilkens, M., "*J. Appl. Cryst.*", Vol. 21, 1988), pp.47-51.
- [23] Ungar, T. S., Sanders Ott, P., Borbely G, A. and Weertman, J. R., "*Acta Mat.*", Vol. 10, 1998) pp.3693-2701.
- [24] Gamal, G. A., Abou Zied, I. M. and Ebnalwaled, A. A., "*Turk J Phys*", Vol. 36, 2012), pp.31-38.
- [25] Blasi, C. De, Micocci, G., Rizzo, A and Tepore, A., "*Physical Review*", Vol. B-27, No. 4, 1983), pp.2429-2458.
- [26] Gamal, G. A, *Semicond. Sci. Technol.*, 12, 1993) 1206-1211.
- [27] Morvavec, F., Sestakova V., Stepanek B, Charvat V., "*Cryst. Res. Technol.*", 24, 3 1989), 275-279.
- [28] Natter H., Schmelzer, M., Loffler, M. S., Krill, A., Fitch, C. E. and Hempelmann, R. J., "*Phys. Chem.*", Vol. B-104, 2000), pp.2467-2472.

## التركيب الدقيق و الخواص الاليكترونية لمركب تيلريد الأنديوم في صورته البلورية

١.د. جمال الدين عطا<sup>١</sup>، د. محمد علي أبوزيد<sup>٢</sup>، د. خالد بن الوليد عبد الفتاح<sup>٢</sup>

<sup>1</sup> أستاذ الفيزياء - كلية الهندسة - جامعة الوصي - المملكة العربية السعودية

<sup>2</sup> قسم الفيزياء - جامعة جنوب الوادي - جمهورية مصر العربية

قدم للنشر في 2111/4/3م - قبل للنشر في 2112/12/11م

ملخص البحث. يتمثل طاقته أشباه الموصلات مكاناً متميزاً في علوم المواد و اليكترونيات أشباه الموصلات عالي حدٍ سواء. وألن البحث اجلاري يُعَمِّن مركب شبه موصل جديدي ( $\text{In}_3\text{Te}_4$ ) فإنه يلزم دراسة خواصه قبل تطبيقه على التطبيق. بُدأ أن هذه الخواص تعتمد بدورها على اخلصائص التركيبية والليكترونية، وعلى ذلك فقد سار البحث وفقاً للخطوات التالية:

• أمكن تحضير المركب في صورته البلورية باستخدام تقنية جديدة تعتمد على طريقة برجرمان

Bridgman technique.

• استخدمت طريقة حيود الأشعة السينية X-ray diffraction لدراسة التركيب البلوري الدقيق

للمركب بُدأ الدراسة.

• تم تفسير نتائج اخلوود للأشعة السينية على ضوء قوانين براج Bragg — Scherrer — وليام

سون هول Williamson — Hall — وارن أفريخ Warren - Averbach المألوفة.

• توصلنا من خلال ما سبق إلى تقييم المركب، ثوابته البلورية lattice parameters، تركيبه،

نظام شبكته، حجم حبيبه grain size، نوع العيوب defects وتوزيعها وكذلك كثافة الإلخناطات

dislocation density ومتوسط المسافة بينها average distance.

• تم ربط النتائج التركيبية باخلصائص الليكترونية للمركب مثل: ظاهرة هول وتركيز حوامل

التيار في وحدة اخلجوم carrier concentration وقابلية التحرك carrier mobility

• نوّشت النتائج السابقة تفصيلاً على النحو الوارد في ممت البحث.